



Crystal plasticity coupled to brittle fracture

November 20th, 2025

11th MFront User Meeting

Jean-Michel Scherer¹, Kaushik Bhattacharya²

¹Centre des Matériaux, Mines Paris

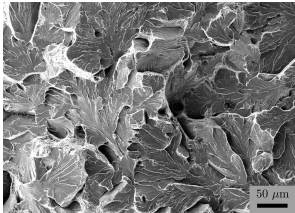
²MCE, Caltech

CONTEXT

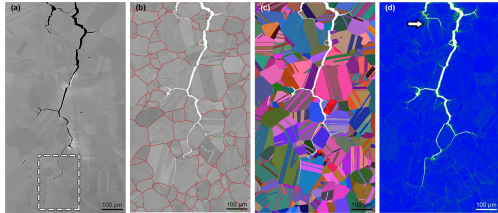
Brittle fracture in polycrystals (metals: W, 3%Si–Fe, steels, ... / ceramics: alumina, magnesia, quartz, ...):

CONTEXT

Brittle fracture in polycrystals (metals: W, 3%Si–Fe, steels, ... / ceramics: alumina, magnesia, quartz, ...):



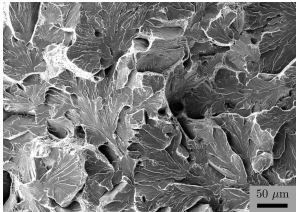
Transgranular brittle fracture showing a "river" pattern
(vgoinc.com/general/fractures-in-the-sem)



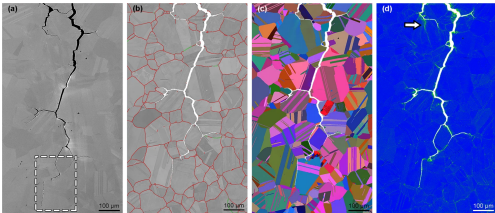
Intergranular brittle fracture in a nickel alloy 725
(Hazarabedian & Iannuzzi, NPJ 2021)

CONTEXT

Brittle fracture in polycrystals (metals: W, 3%Si–Fe, steels, ... / ceramics: alumina, magnesia, quartz, ...):



Transgranular brittle fracture showing a "river" pattern
(vgoinc.com/general/fractures-in-the-sem)

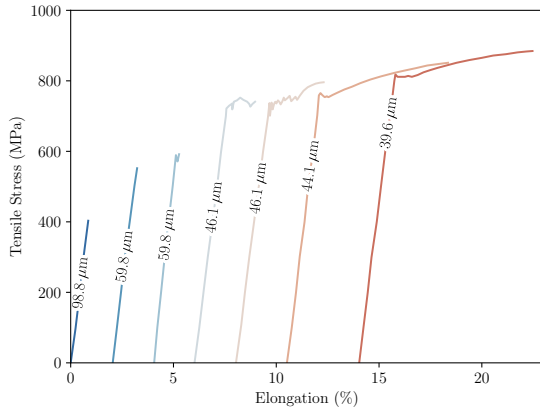


Intergranular brittle fracture in a nickel alloy 725
(Hazarabedian & Iannuzzi, NPJ 2021)

- ▶ Anisotropy of elastic properties: stress concentrations at grain boundaries and triple junctions
- ▶ Heterogeneity of the fracture toughness: crystal bulk vs grain boundary
- ▶ Anisotropy of the fracture toughness: cleavage planes

CONTEXT: PLASTICITY-ASSISTED CRACK NUCLEATION

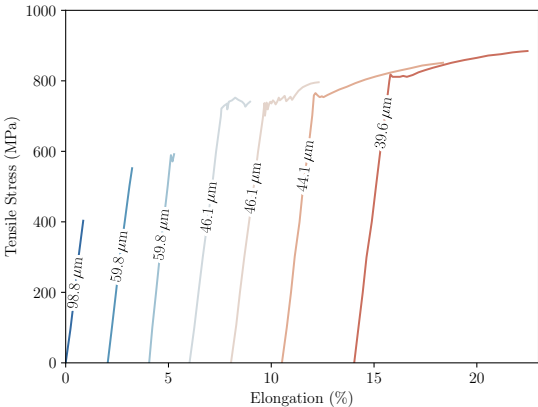
Brittle crack nucleation can be assisted by plasticity:



Tensile behaviour of 3%Si – iron for different grain sizes
(Hull, Acta. Metall. 1961)

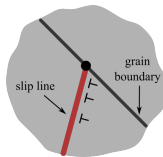
CONTEXT: PLASTICITY-ASSISTED CRACK NUCLEATION

Brittle crack nucleation can be assisted by plasticity:

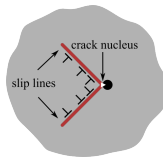


Tensile behaviour of 3%Si – iron for different grain sizes
(Hull, Acta. Metall. 1961)

Mechanisms involved in the plasticity-assisted crack nucleation:



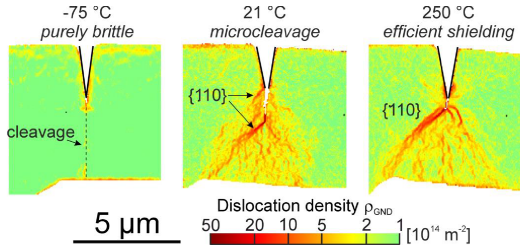
Slip line arrested at a grain boundary
(Stroh, Adv. in Phy. 1957)



Intersecting slip lines
(Cottrell, Tr. Metall. Soc. 1958)

CONTEXT: PLASTICITY-IMPEDED CRACK PROPAGATION

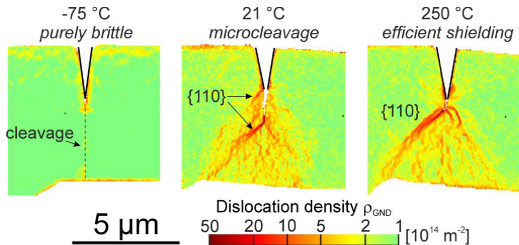
Brittle crack propagation can be impeded by plasticity:



Fracture of tungsten microcantilevers
(Ast *et al.*, Mat. & Design 2018)

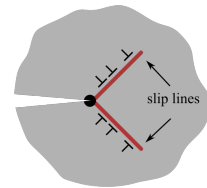
CONTEXT: PLASTICITY-IMPEDED CRACK PROPAGATION

Brittle crack propagation can be impeded by plasticity:



Fracture of tungsten microcantilevers
(Ast *et al.*, Mat. & Design 2018)

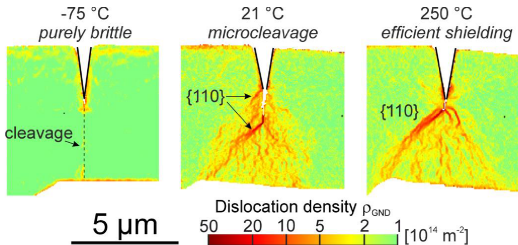
Mechanism involved in the plasticity-impeded crack propagation:



Plastic zone at the crack tip
(Rice & Thomson, Phil. Mag. A 1974)

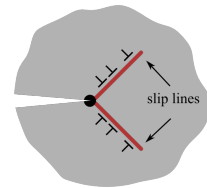
CONTEXT: PLASTICITY-IMPEDED CRACK PROPAGATION

Brittle crack propagation can be impeded by plasticity:



Fracture of tungsten microcantilevers
(Ast *et al.*, Mat. & Design 2018)

Mechanism involved in the plasticity-impeded crack propagation:



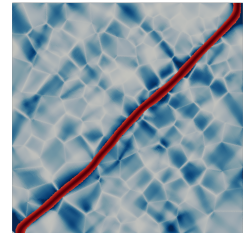
Plastic zone at the crack tip
(Rice & Thomson, Phil. Mag. A 1974)

- ▶ plasticity-induced crack nucleation: dislocation pile-ups
- ▶ plasticity-shielded crack propagation: crack tip blunting
- ▶ plasticity-affected crack path: crack deflection

OBJECTIVE AND OUTLINE

Extend the variational approach to fracture to the problem of plasticity-assisted fracture of brittle polycrystals in order to account for:

- ▶ crack nucleation and propagation
- ▶ grain size effects (Hall-Petch)
- ▶ plasticity-affected crack paths



A phase-field model coupled to crystal plasticity

Finite element implementation

Crack nucleation

Crack propagation

Conclusion & Outlook

A PHASE-FIELD MODEL COUPLED TO CRYSTAL PLASTICITY

- Phase-field regularization of the total energy of an elasto-plastic polycrystal Ω (JMS & et al., JMPS 2024)

$$\begin{aligned}\mathcal{E}(E_{\text{GL}}^e, \gamma^s, \alpha) = & \int_{\Omega} \frac{(1-\alpha)^2}{2} E_{\text{GL}}^e : \mathbb{C} : E_{\text{GL}}^e \, dx + \int_{\Omega} (1-\alpha)^2 \int_0^{\bar{t}} \sum_{s=1}^N \tau^s \dot{\gamma}^s dt \, dx \\ & + \int_{\Omega} \frac{3G_c}{8\ell} (\alpha + \ell^2 |\nabla \alpha|^2) \, dx - \int_{\partial \Omega_t} \mathbf{f} \cdot \mathbf{u} \, dx\end{aligned}$$

A PHASE-FIELD MODEL COUPLED TO CRYSTAL PLASTICITY

- Phase-field regularization of the total energy of an elasto-plastic polycrystal Ω (JMS & et al., JMPS 2024)

$$\begin{aligned}\mathcal{E}(E_{\text{GL}}^e, \gamma^s, \alpha) = & \int_{\Omega} \frac{(1-\alpha)^2}{2} E_{\text{GL}}^e : \mathbb{C} : E_{\text{GL}}^e \, dx + \int_{\Omega} (1-\alpha)^2 \int_0^{\bar{t}} \sum_{s=1}^N \tau^s \dot{\gamma}^s dt \, dx \\ & + \int_{\Omega} \frac{3G_c}{8\ell} (\alpha + \ell^2 |\nabla \alpha|^2) \, dx - \int_{\partial \Omega_t} \mathbf{f} \cdot \mathbf{u} \, dx\end{aligned}$$

- Finite strain crystal plasticity behaviour

$$F = F^e \cdot F^p \quad \text{and} \quad E_{\text{GL}}^e = \frac{1}{2} (F^{e^T} \cdot F^e - I)$$

$$\dot{F}^p \cdot F^{p^{-1}} = \sum_{s=1}^N \dot{\gamma}^s m^s \otimes n^s$$

A PHASE-FIELD MODEL COUPLED TO CRYSTAL PLASTICITY

- Phase-field regularization of the total energy of an elasto-plastic polycrystal Ω (JMS & et al., JMPS 2024)

$$\begin{aligned}\mathcal{E}(E_{\text{GL}}^e, \gamma^s, \alpha) = & \int_{\Omega} \frac{(1-\alpha)^2}{2} E_{\text{GL}}^e : \mathbb{C} : E_{\text{GL}}^e \, dx + \int_{\Omega} (1-\alpha)^2 \int_0^{\bar{t}} \sum_{s=1}^N \tau^s \dot{\gamma}^s dt \, dx \\ & + \int_{\Omega} \frac{3G_c}{8\ell} (\alpha + \ell^2 |\nabla \alpha|^2) \, dx - \int_{\partial \Omega_t} \mathbf{f} \cdot \mathbf{u} \, dx\end{aligned}$$

- Finite strain crystal plasticity behaviour

$$F = F^e \cdot F^p \quad \text{and} \quad E_{\text{GL}}^e = \frac{1}{2} (F^{e^T} \cdot F^e - I)$$

$$\Pi^M = F^{e^T} \cdot F^e \cdot \Pi^e = F^{e^T} \cdot F^e \cdot \mathbb{C} : E_{\text{GL}}^e$$

$$\dot{F}^p \cdot F^{p^{-1}} = \sum_{s=1}^N \dot{\gamma}^s m^s \otimes n^s$$

$$\tau^s = \Pi^M : (m^s \otimes n^s) \quad \text{and} \quad \dot{\gamma}^s = \dot{\gamma}_0 \left\langle \frac{|\tau^s| - \tau_c^s}{\tau_0} \right\rangle^n$$

DISLOCATION-DENSITY BASED CRYSTAL PLASTICITY

- Dislocation-density based crystal plasticity model for BCC materials

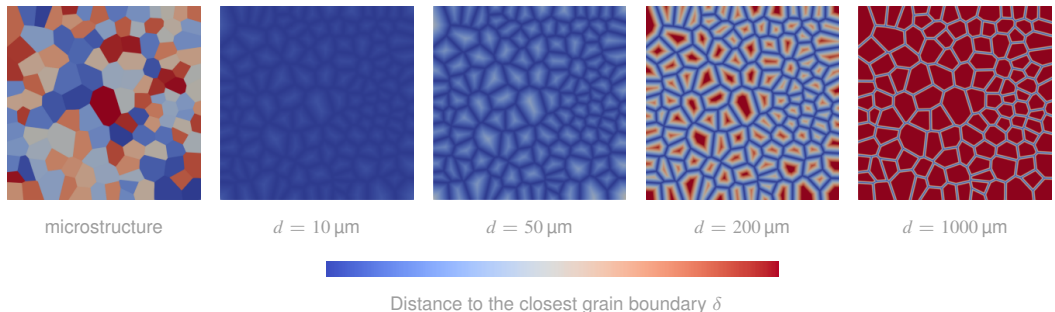
$$\tau_c^s = \tau_0 + \mu b \sqrt{\sum_{u=1}^{24} a^{su} \rho^u} \quad \text{and} \quad \dot{\rho}^s = \frac{|\dot{\gamma}^s|}{b} \left(\max \left(\frac{K_s}{\delta}, \frac{\sqrt{\sum_{u \notin \text{coplanar}(s)} a^{su} \rho^u}}{K_{\text{obstacle}}} + \frac{\sqrt{\sum_{u \in \text{coplanar}(s)} a^{su} \rho^u}}{K_{\text{coplanar}}} \right) - y b \rho^s \right)$$

DISLOCATION-DENSITY BASED CRYSTAL PLASTICITY

- Dislocation-density based crystal plasticity model for BCC materials

$$\tau_c^s = \tau_0 + \mu b \sqrt{\sum_{u=1}^{24} a^{su} \rho^u} \quad \text{and} \quad \dot{\rho}^s = \frac{|\dot{\gamma}^s|}{b} \left(\max \left(\frac{K_s}{\delta}, \frac{\sqrt{\sum_{u \notin \text{coplanar}(s)} a^{su} \rho^u}}{K_{\text{obstacle}}} + \frac{\sqrt{\sum_{u \in \text{coplanar}(s)} a^{su} \rho^u}}{K_{\text{coplanar}}} \right) - y b \rho^s \right)$$

- Hall-Petch effect modeled through the term K_s/δ (Haouala *et al.*, JMPS 2020)



FINITE ELEMENT IMPLEMENTATION: MFRONT, MGIS.FENICS, FENICS

- Mechanical and phase-field weak forms are implemented in FEniCS (staggered resolution scheme):

<https://github.com/jeanmichelscherer/GRADAM>

```
1 # Definition of energy densities
2 self.Wel = (1.-self.d)**2* self.stored* self.dx
3 self.Wdis = (1.-self.d)**2* self.dissipated* self.dx
4 self.Efrac = self.mat.fracture_energy_density(self.d, self.d_prev_iter)
5 self.Wfrac = sum(self.Efrac)* self.dx
6 self.Wtot = self.Wel + self.Wdis + self.Wfrac - self.Wext
7
8 # Definition of energy derivatives
9 self.DW_u = derivative(self.Wtot, self.u, self.u_)
10 self.D2W_u = derivative(self.DW_u, self.u, self.du)
11 self.DW_d = derivative(self.Wtot, self.d, self.d_)
12 self.D2W_d = derivative(self.DW_d, self.d, self.dd)
13
14 # Definition of solvers
15 self.solver_u = mf.MFrontNonlinearProblem(self.u, self.mb, quadrature_degree=self.qd, bcs=self.bcs)
16 self.solver_u.solver = PETScSNESSolver('newtontr')
17 self.solver_u.solver.parameters['linear_solver'] = 'gmres'
18 self.solver_u.solver.parameters['preconditioner'] = 'amg'
19 self.solver_d = PETScTAOSolver()
20 self.solver_d.parameters["method"] = "tron"
21 self.solver_d.parameters["linear_solver"] = "cg"
22
23 # Solve
24 self.niter_u += self.solver_u.solve(self.u.vector())
25 dam_prob = DamageProblem(self.Wtot, self.DW_d, self.D2W_d, self.d)
26 self.niter_d += self.solver_d.solve(dam_prob, self.d.vector(), self.d_lb.vector(), self.d_ub.vector())[0]
```

FINITE ELEMENT IMPLEMENTATION: MFRONT, MGIS . FENICS, FENICS

- ▶ Mechanical and phase-field weak forms are implemented in FEniCS (staggered resolution scheme):
<https://github.com/jeanmichelscherer/GRADAM>
- ▶ Crystal plasticity constitutive behaviour is implemented in MFront:
Scherer, Jean-Michel; Bhattacharya, Kaushik, 2025, "MFront implementation of a BCC crystal plasticity law coupled to phase-field damage", <https://doi.org/10.57745/IUXPA3>, Recherche Data Gouv, V1

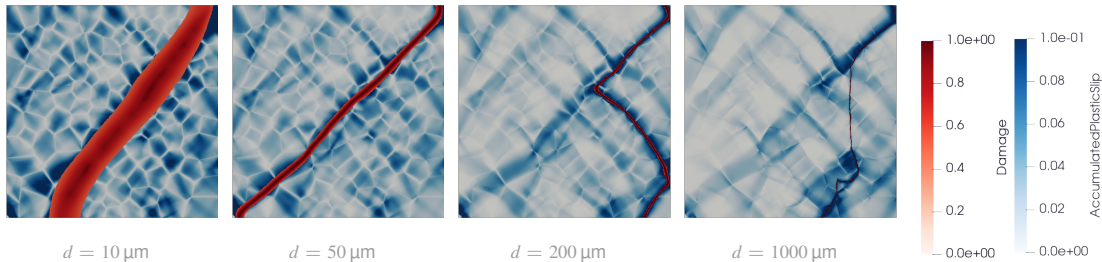
FINITE ELEMENT IMPLEMENTATION: MFRONT, MGIS . FENICS, FENICS

- ▶ Mechanical and phase-field weak forms are implemented in FEniCS (staggered resolution scheme):
<https://github.com/jeanmichelscherer/GRADAM>
- ▶ Crystal plasticity constitutive behaviour is implemented in MFront:
Scherer, Jean-Michel; Bhattacharya, Kaushik, 2025, "MFront implementation of a BCC crystal plasticity law coupled to phase-field damage", <https://doi.org/10.57745/IUXPA3>, Recherche Data Gouv, V1
- ▶ The interface between FEniCS and MFront is handled via mgis.fenics:

```
1 import mgis.fenics as mf
2
3 class MfrontBehaviour:
4     def create_material(self):
5         material = mf.MFrontNonlinearMaterial(self.mfront_library,
6                                              self.behaviour,
7                                              hypothesis=self.hypothesis,
8                                              material_properties=self.mat_prop,
9                                              rotation_matrix=self.rotation_matrix)
10    class Problem:
11        def __init__(self, ...):
12            self.mb = self.mat.mfrontBehaviour.create_material()
13            self.solver_u = mf.MFrontNonlinearProblem(self.u, self.mb, quadrature_degree=self.qd, bcs=self.bcs)
14            self.solver_u.register_external_state_variable("Damage", self.d)
```

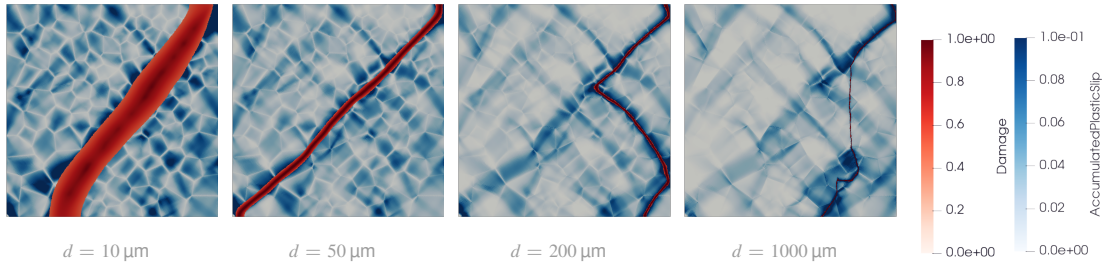
CRACK NUCLEATION: 2D PLANE STRAIN TENSILE TEST

- ▶ Accumulated plastic slip and damage fields at the onset of crack nucleation in a tensile test in the horizontal direction for several grain sizes (JMS *et al.*, JMPS 2025)



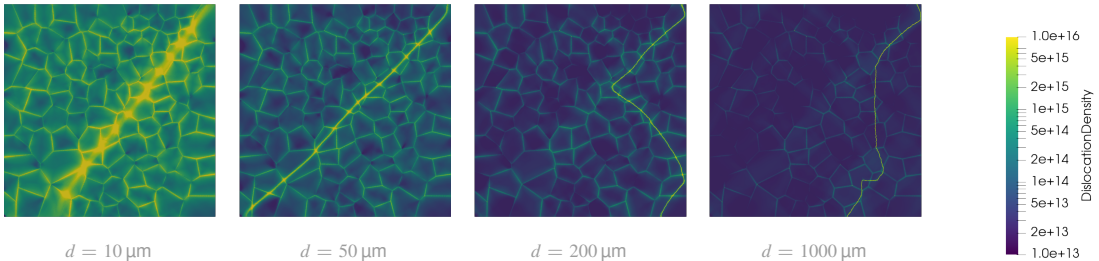
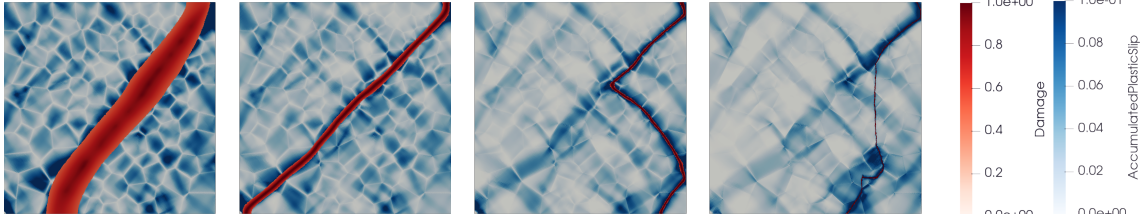
CRACK NUCLEATION: 2D PLANE STRAIN TENSILE TEST

- ▶ Accumulated plastic slip and damage fields at the onset of crack nucleation in a tensile test in the horizontal direction for several grain sizes (JMS *et al.*, JMPS 2025)

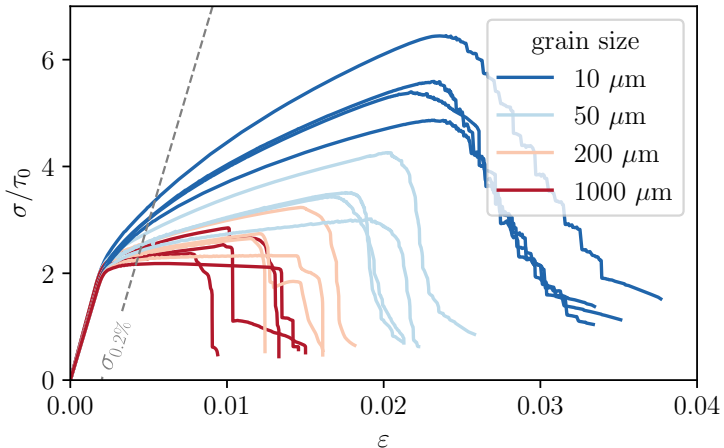


- ▶ Cracks nucleate in regions of high elastic energy density / plastic dissipation: triple junctions, grain boundaries
- ▶ Plasticity and phase fields are more diffuse for fine grain microstructures
- ▶ Abrupt changes of direction in the crack path are observed for larger grain sizes

CRACK NUCLEATION: 2D PLANE STRAIN TENSILE TEST



CRACK NUCLEATION: 2D PLANE STRAIN TENSILE TEST



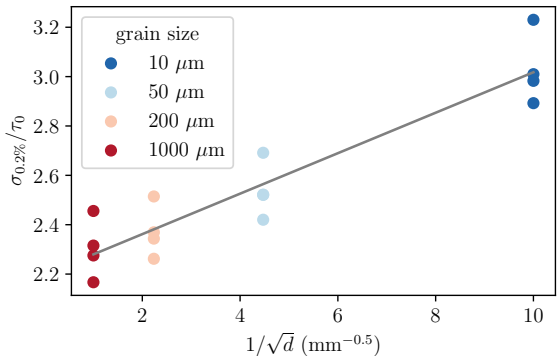
Stress vs strain curves for several microstructures with different grain sizes

CRACK NUCLEATION: 2D PLANE STRAIN TENSILE TEST

- The yield strength and fracture strength follow the Hall-Petch law $\sigma = \sigma_\infty + k/\sqrt{d}$

CRACK NUCLEATION: 2D PLANE STRAIN TENSILE TEST

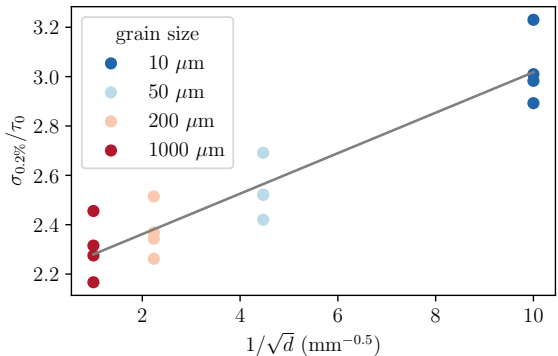
- The yield strength and fracture strength follow the Hall-Petch law $\sigma = \sigma_\infty + k/\sqrt{d}$



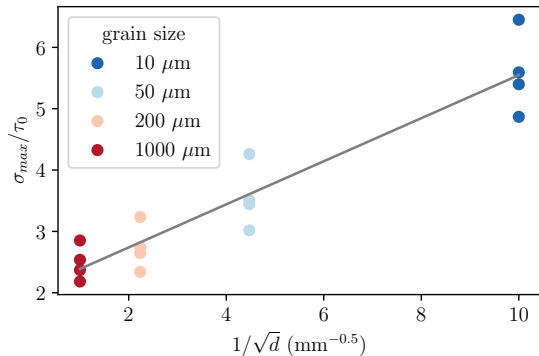
Yield strength as a function of the grain size

CRACK NUCLEATION: 2D PLANE STRAIN TENSILE TEST

- The yield strength and fracture strength follow the Hall-Petch law $\sigma = \sigma_\infty + k/\sqrt{d}$

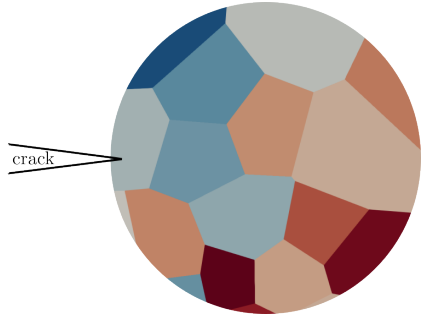


Yield strength as a function of the grain size



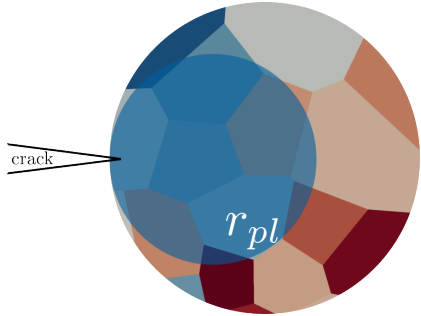
Fracture strength as a function of the grain size

CRACK PROPAGATION: PLASTIC AND PROCESS ZONES



Schematic representation of the plastic and process zones in a polycrystal

CRACK PROPAGATION: PLASTIC AND PROCESS ZONES



Schematic representation of the plastic and process zones in a polycrystal

► Plastic zone size

$$r_{pl} \propto \frac{E' G_c}{\tau_0^2}$$

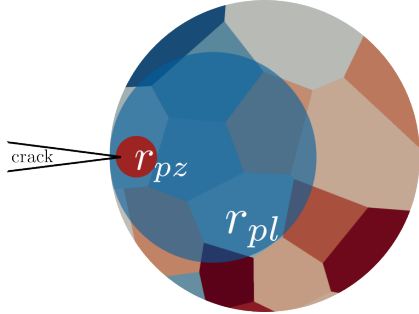
► Process zone size

$$r_{pz} \propto \frac{G_c}{\tau_0}$$

► Relative size of the plastic and process zones

$$q = \frac{r_{pl}}{r_{pz}} \propto \frac{E'}{\tau_0} \gg 1$$

CRACK PROPAGATION: PLASTIC AND PROCESS ZONES



Schematic representation of the plastic and process zones in a polycrystal

► Plastic zone size

$$r_{\text{pl}} \propto \frac{E' G_c}{\tau_0^2}$$

► Process zone size

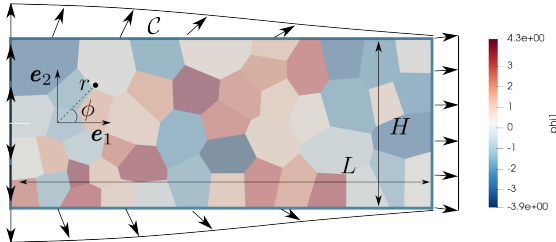
$$r_{\text{pz}} \propto \frac{G_c}{\tau_0}$$

► Relative size of the plastic and process zones

$$q = \frac{r_{\text{pl}}}{r_{\text{pz}}} \propto \frac{E'}{\tau_0} \gg 1$$

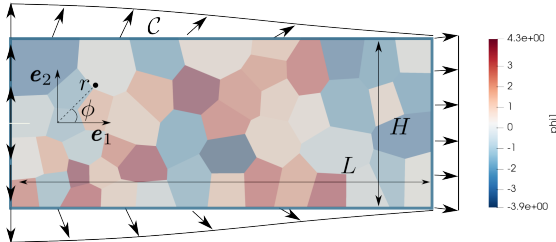
CRACK PROPAGATION: SURFING BOUNDARY CONDITIONS

Surfing boundary conditions modelling mode I crack propagation at velocity v_0



CRACK PROPAGATION: SURFING BOUNDARY CONDITIONS

Surfing boundary conditions modelling mode I crack propagation at velocity v_0

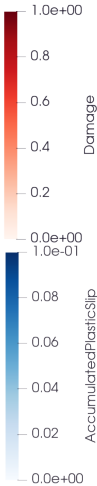
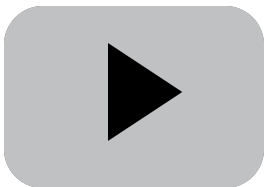


$$\mathbf{u}(\mathbf{x}, t) = \mathbf{U}(\mathbf{x} - v_0 t \mathbf{e}_1) = \psi \sqrt{\frac{(1 + \nu) G_c}{2E}} (3 - 4\nu - \cos \phi) \sqrt{\frac{r}{2\pi}} \left(\cos\left(\frac{\phi}{2}\right) \mathbf{e}_1 + \sin\left(\frac{\phi}{2}\right) \mathbf{e}_2 \right)$$

$$r(\mathbf{x}, t) = \sqrt{(x - x_0 - v_0 t)^2 + (y - y_0)^2} \quad \text{and} \quad \theta(\mathbf{x}, t) = \arctan\left(\frac{y - y_0}{x - x_0 - v_0 t}\right)$$

CRACK PROPAGATION (JMS *et al.*, JMPS 2025)

- phase-field and accumulated plastic slip ($r_{pl}/r_{pz} = 2.5 \times 10^2$, $d = 200 \mu\text{m}$)



CRACK PROPAGATION: EFFECT OF THE DUCTILITY ($r_{pl}/r_{pz} = 2.5 \times 10^2$)

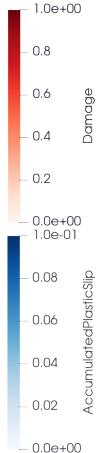
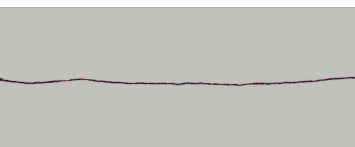
$d = 50 \mu\text{m}$



$d = 200 \mu\text{m}$

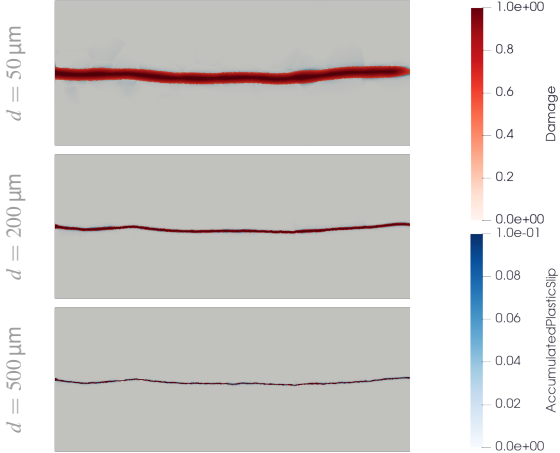


$d = 500 \mu\text{m}$



Damage

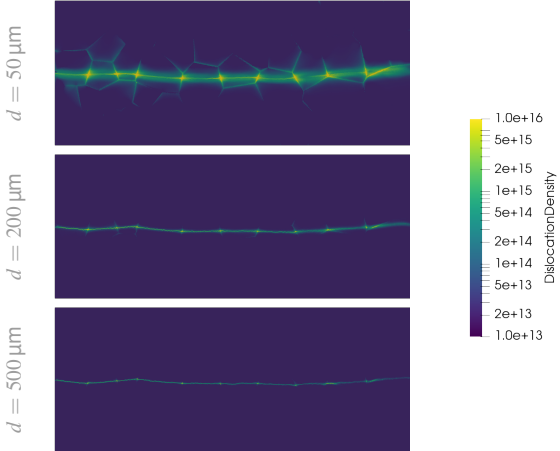
CRACK PROPAGATION: EFFECT OF THE DUCTILITY ($r_{pl}/r_{pz} = 2.5 \times 10^2$)



For a low ductility:

- ▶ The plastic activity is contained in a single layer of grains above and below the crack path
- ▶ Microstructures with larger grain sizes display an almost elastic-brittle behaviour
- ▶ Small deflections of the crack at grain boundaries are due to the elastic anisotropy rather than plasticity

CRACK PROPAGATION: EFFECT OF THE DUCTILITY ($r_{pl}/r_{pz} = 2.5 \times 10^2$)

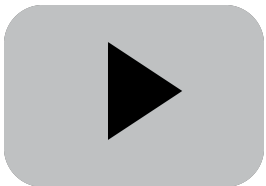


For a low ductility:

- ▶ The plastic activity is contained in a single layer of grains above and below the crack path
- ▶ Microstructures with larger grain sizes display an almost elastic-brittle behaviour
- ▶ Small deflections of the crack at grain boundaries are due to the elastic anisotropy rather than plasticity

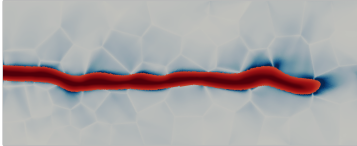
CRACK PROPAGATION (JMS *et al.*, JMPS 2025)

- phase-field and accumulated plastic slip ($r_{pl}/r_{pz} = 5 \times 10^2$, $d = 200 \mu\text{m}$)



CRACK PROPAGATION: EFFECT OF THE DUCTILITY ($r_{pl}/r_{pz} = 5 \times 10^2$)

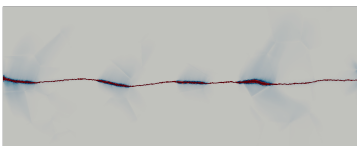
$d = 50 \mu\text{m}$



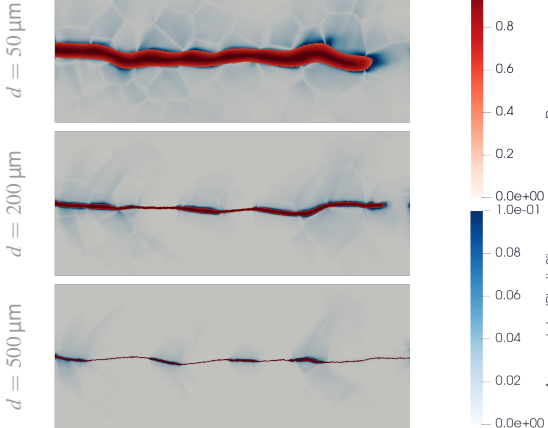
$d = 200 \mu\text{m}$



$d = 500 \mu\text{m}$



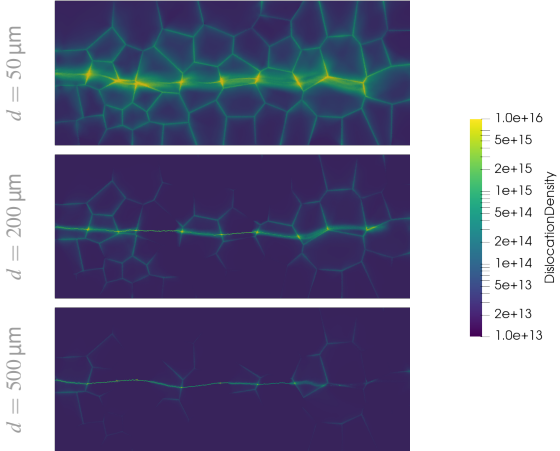
CRACK PROPAGATION: EFFECT OF THE DUCTILITY ($r_{pl}/r_{pz} = 5 \times 10^2$)



For an intermediate ductility:

- ▶ Jerky crack growth: incubation periods followed by crack jumps
- ▶ The crack paths are more tortuous than for a lower ductility
- ▶ Crack jumps occur on distances comparable to the grain size. Grain boundaries interrupt unstable crack growth
- ▶ Crack jumps occur predominantly in the microstructure with larger grains

CRACK PROPAGATION: EFFECT OF THE DUCTILITY ($r_{pl}/r_{pz} = 5 \times 10^2$)



For an intermediate ductility:

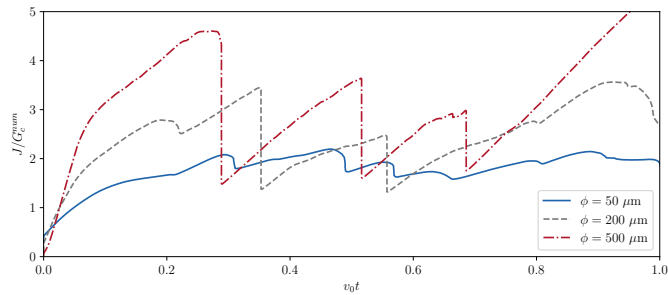
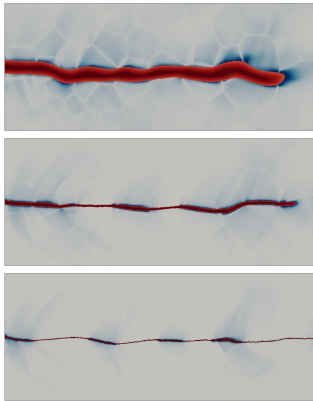
- ▶ Jerky crack growth: incubation periods followed by crack jumps
- ▶ The crack paths are more tortuous than for a lower ductility
- ▶ Crack jumps occur on distances comparable to the grain size. Grain boundaries interrupt unstable crack growth
- ▶ Crack jumps occur predominantly in the microstructure with larger grains

CRACK PROPAGATION: EFFECT OF THE GRAIN SIZE (J-INTEGRALS)

- The J-integral is computed over a contour Γ surrounding the crack tip

$$J = \int_{\Gamma} ((\mathbf{E} : a(\alpha) \mathbb{C} : \mathbf{E}) \mathbf{1} - \nabla \mathbf{u}^T : a(\alpha) \mathbb{C} : \mathbf{E}) \cdot \mathbf{n} \, ds$$

$d = 500 \mu m$ $d = 200 \mu m$ $d = 50 \mu m$



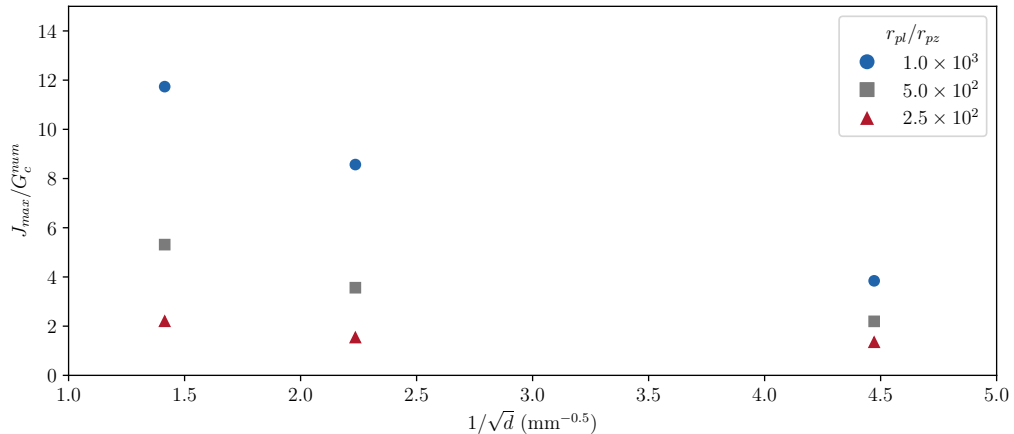
J-integral as a function of the grain size for $q = r_{p1}/r_{pz} = 5 \times 10^2$

CRACK PROPAGATION: INVERSE HALL-PETCH SIZE EFFECT

- The apparent fracture toughness J_{max} follows an inverse Hall-Petch law

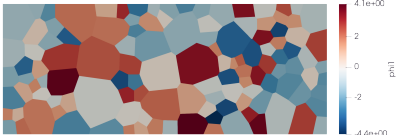
CRACK PROPAGATION: INVERSE HALL-PETCH SIZE EFFECT

- The apparent fracture toughness J_{max} follows an inverse Hall-Petch law

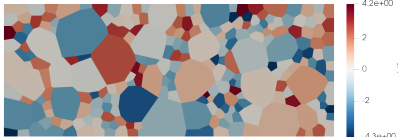


CRACK PROPAGATION: EFFECT OF BIMODAL GRAIN SIZE DISTRIBUTION

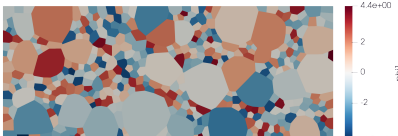
$$d_1/d_2 = 2$$



$$d_1/d_2 = 3$$

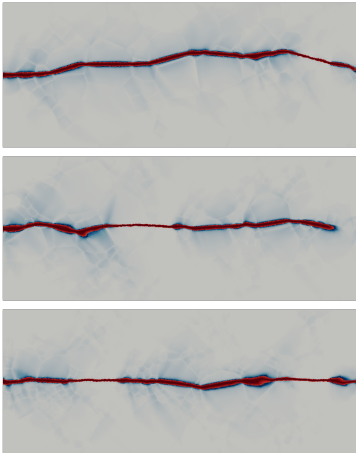


$$d_1/d_2 = 4$$



CRACK PROPAGATION: EFFECT OF BIMODAL GRAIN SIZE DISTRIBUTION

$d_1/d_2 = 2$



For a bimodal grain size distribution:

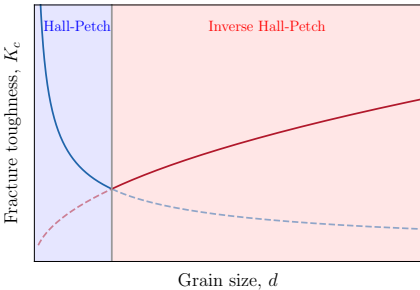
- ▶ Crack path is more tortuous with larger secondary grains
- ▶ Dislocation density is highest in the small grains population
- ▶ Large grains induces crack tip blunting and increases significantly the overall fracture toughness
- ▶ Increased scatter (Chakrabarti *et al.*, Met. Mater. Trans 2009)

CONCLUSION & OUTLOOK

- ▶ Crystal plasticity coupled with phase-field model of fracture
- ▶ Crack nucleation follows a Hall-Petch size effect
- ▶ Fracture toughness follows an inverse Hall-Petch size effect

CONCLUSION & OUTLOOK

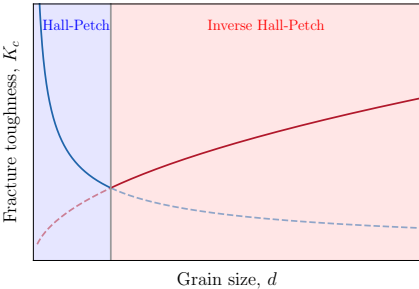
- ▶ Crystal plasticity coupled with phase-field model of fracture
- ▶ Crack nucleation follows a Hall-Petch size effect
- ▶ Fracture toughness follows an inverse Hall-Petch size effect



Apparent fracture toughness as a function of the grain size (Reiser & Hartmaier, Sci. Rep. 2020)

CONCLUSION & OUTLOOK

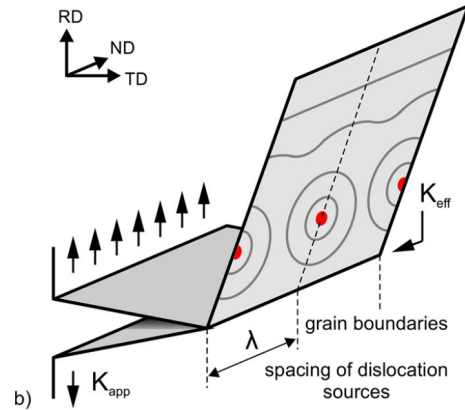
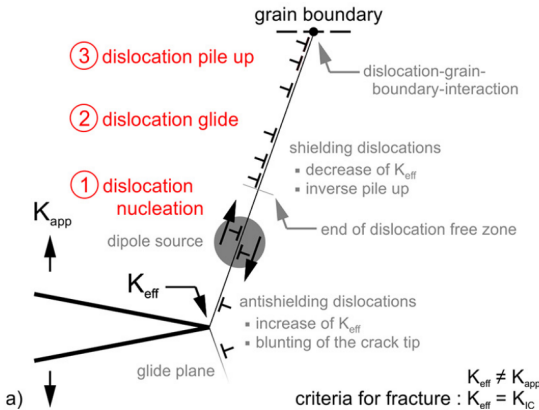
- ▶ Crystal plasticity coupled with phase-field model of fracture
- ▶ Crack nucleation follows a Hall-Petch size effect
- ▶ Fracture toughness follows an inverse Hall-Petch size effect



Apparent fracture toughness as a function of the grain size (Reiser & Hartmaier, Sci. Rep. 2020)

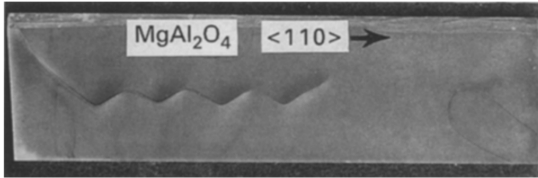
- ▶ Account for intergranular fracture: heterogeneous fracture toughness
- ▶ Account for anisotropic fracture: cleavage planes
(Scherer *et al.*, CMAME 2021)

NON-MONOTONIC DEPENDENCE OF FRACTURE TOUGHNESS ON GRAIN SIZE



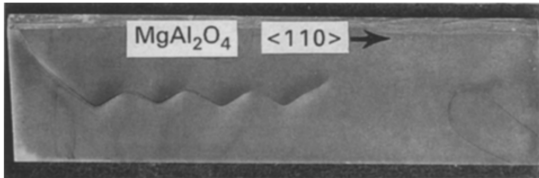
Schematic representation of crack tip plasticity (Bonnekoh *et al.*, Int. J. of Ref. Met. & Hard Mat 2019)

CONTEXT: CLEAVAGE PLANES

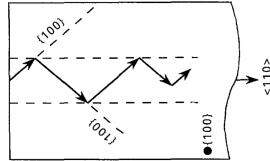


Intergranular crack wandering in a MgAl₂O₄ single crystal
(Wu *et al.*, JMSL 1995)

CONTEXT: CLEAVAGE PLANES

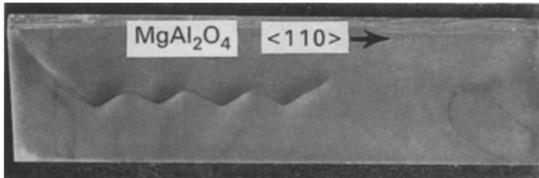


Intergranular crack wandering in a MgAl_2O_4 single crystal
(Wu *et al.*, JMSL 1995)

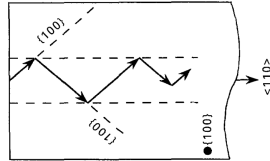


{100} cleavage planes in a MgAl_2O_4 single crystal
(Wu *et al.*, JMSL 1995)

CONTEXT: CLEAVAGE PLANES



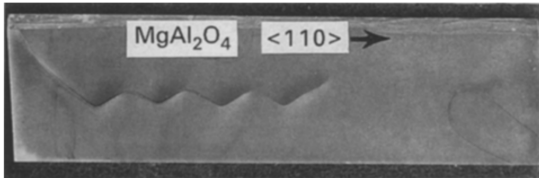
Intergranular crack wandering in a MgAl_2O_4 single crystal
(Wu *et al.*, JMSL 1995)



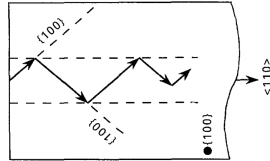
{100} cleavage planes in a MgAl_2O_4 single crystal
(Wu *et al.*, JMSL 1995)

- ▶ Crack path follows {100} planes in {100} spinel plates

CONTEXT: CLEAVAGE PLANES

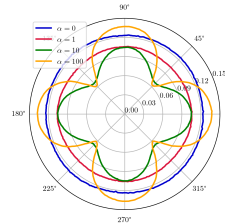


Intergranular crack wandering in a MgAl₂O₄ single crystal
(Wu *et al.*, JMSL 1995)



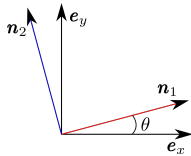
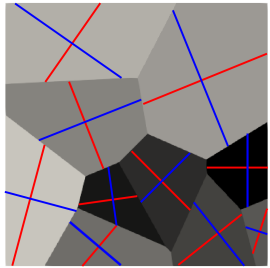
{100} cleavage planes in a MgAl₂O₄ single crystal
(Wu *et al.*, JMSL 1995)

- ▶ Crack path follows {100} planes in {100} spinel plates
- ▶ Suggests that fracture toughness is anisotropic



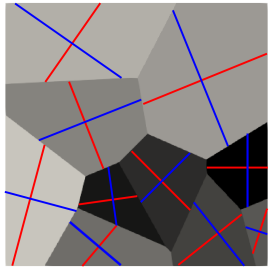
Weak and strong anisotropic surface energy (JMS *et al.*, CMAME 2022)

MULTI-PHASE-FIELD MODELS OF CLEAVAGE FRACTURE

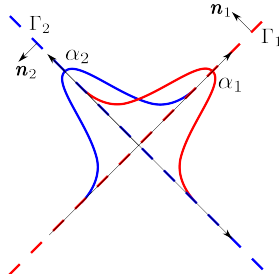
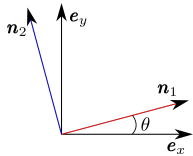


Microstructure of a polycrystalline material with two cleavage planes

MULTI-PHASE-FIELD MODELS OF CLEAVAGE FRACTURE

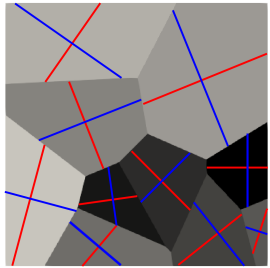


Microstructure of a polycrystalline material with two cleavage planes

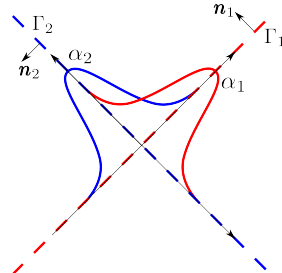
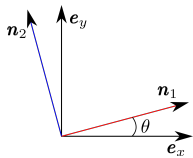


Phase-field profiles on cleavage planes n_1 and n_2

MULTI-PHASE-FIELD MODELS OF CLEAVAGE FRACTURE



Microstructure of a polycrystalline material with two cleavage planes



Phase-field profiles on cleavage planes n_1 and n_2

- ▶ Multi-phase-field regularization of the total energy of an elastic polycrystal with cleavage planes

$$\mathcal{E}(u, \alpha_i) = \int_{\Omega} \frac{1}{2} \boldsymbol{\varepsilon} : \mathbb{C}(\alpha_i) : \boldsymbol{\varepsilon} dx + \int_{\Omega} \sum_{i=1}^n \frac{3G_c^i}{8} \left(\frac{\alpha_i}{\ell_i} + \ell_i \mathbf{B}_i : (\nabla \alpha_i \otimes \nabla \alpha_i) \right) dx - \int_{\partial \Omega_t} f \cdot u dx$$

AFE vs ASD MODELS (JMS *et al.*, CMAME 2022)

$$\mathcal{E}(u, \alpha_i) = \int_{\Omega} \frac{1}{2} \boldsymbol{\varepsilon} : \mathbb{C}(\alpha_i) : \boldsymbol{\varepsilon} \, dx + \int_{\Omega} \sum_{i=1}^n \frac{3G_c^i}{8} \left(\frac{\alpha_i}{\ell_i} + \ell_i \mathbf{B}_i : (\nabla \alpha_i \otimes \nabla \alpha_i) \right) \, dx - \int_{\partial \Omega_t} f \cdot u \, dx$$

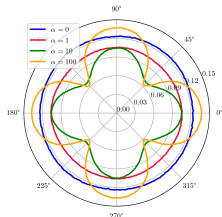
AFE vs ASD MODELS (JMS et al., CMAME 2022)

$$\mathcal{E}(u, \alpha_i) = \int_{\Omega} \frac{1}{2} \boldsymbol{\varepsilon} : \mathbb{C}(\alpha_i) : \boldsymbol{\varepsilon} dx + \int_{\Omega} \sum_{i=1}^n \frac{3G_c^i}{8} \left(\frac{\alpha_i}{\ell_i} + \ell_i \mathbf{B}_i : (\nabla \alpha_i \otimes \nabla \alpha_i) \right) dx - \int_{\partial \Omega_t} f \cdot u dx$$

Anisotropic fracture energy (AFE)

$$\mathbf{B}_i = \mathbf{1} + \beta_i (\mathbf{1} - \mathbf{n}_i \otimes \mathbf{n}_i)$$

$$\mathbb{C}(d_i) = \left((1 - \kappa) \prod_{i=1}^n (1 - d_i)^2 + \kappa \right) \mathbb{C}_0$$



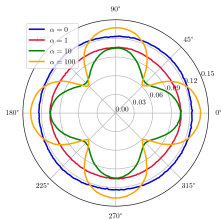
AFE vs ASD MODELS (JMS et al., CMAME 2022)

$$\mathcal{E}(u, \alpha_i) = \int_{\Omega} \frac{1}{2} \boldsymbol{\varepsilon} : \mathbb{C}(\alpha_i) : \boldsymbol{\varepsilon} dx + \int_{\Omega} \sum_{i=1}^n \frac{3G_c^i}{8} \left(\frac{\alpha_i}{\ell_i} + \ell_i \mathbf{B}_i : (\nabla \alpha_i \otimes \nabla \alpha_i) \right) dx - \int_{\partial \Omega_t} f \cdot u dx$$

Anisotropic fracture energy (AFE)

$$\mathbf{B}_i = \mathbf{1} + \beta_i (\mathbf{1} - \mathbf{n}_i \otimes \mathbf{n}_i)$$

$$\mathbb{C}(d_i) = \left((1 - \kappa) \prod_{i=1}^n (1 - d_i)^2 + \kappa \right) \mathbb{C}_0$$



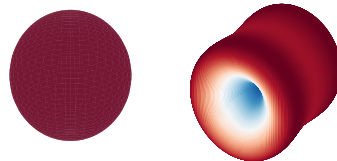
Anisotropic stiffness degradation (ASD)

$$\mathbf{B}_i = \mathbf{1}$$

$$\mathbb{C}(d_1, d_2) = \mathbb{D} : \mathbb{C}_0 : \mathbb{D}$$

$$= \begin{pmatrix} g_1^2 C_{11} & g_1 g_2 C_{12} & 0 \\ g_1 g_2 C_{12} & g_2^2 C_{22} & 0 \\ 0 & 0 & g_6^2 C_{66} \end{pmatrix}$$

Young's modulus $E(\mathbf{d})$



AFE vs ASD MODELS (JMS *et al.*, CMAME 2022)

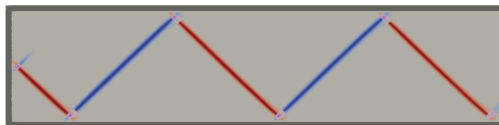
AFE-1



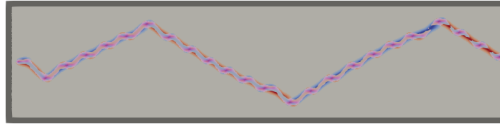
AFE-10



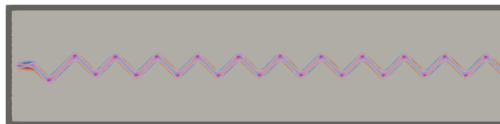
AFE-100



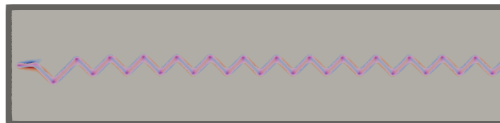
ASD-(1, 1, 2)



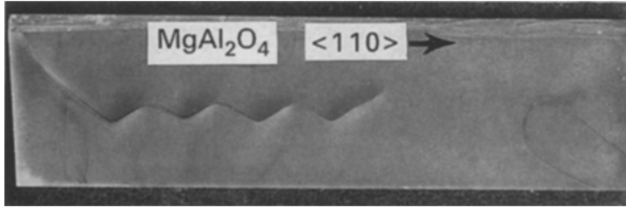
ASD-(1, 1, 3)



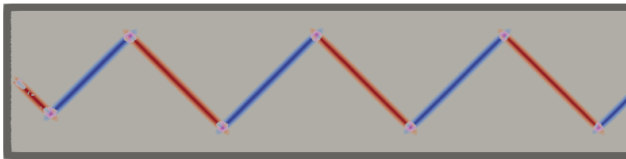
ASD-(1, 1, 4)



COMBINING FRACTURE ENERGY AND STIFFNESS ANISOTROPIES

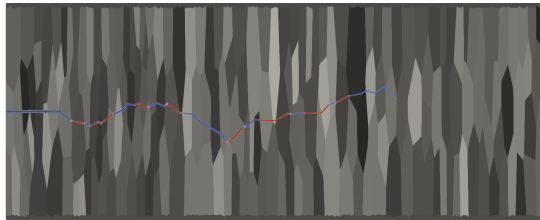
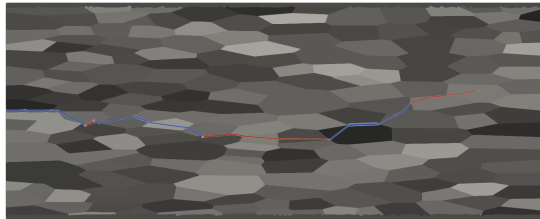


Intergranular crack wandering in a MgAl_2O_4 single crystal
(Wu *et al.*, JMSL 1995)



Model combining anisotropic fracture energy and anisotropic stiffness degradation

FRACTURE TOUGHNESS OF POLYCRYSTALS: TEXTURE EFFECTS



Crack paths in textured synthetic polycrystals